Received: 23/7/2025 | Accepted: 17/9/2025 | Published: 30/1/2026

CONTEMPORARY RESEARCH IN NATURAL PRODUCTS

Article

Multifaceted Evaluation of Acetophenones: From RSM-Assisted Optimization to In Vivo Depigmentation and Molecular Docking Validation

Nik Nur Farhana Nik Aizan[1], Muhammad Syafiq Akmal Mohd Fahmi[2], Siti Nurulhuda Mastuki[2,3], Siti Efliza Ashari[4], and Siti Munirah Mohd Faudzi,[1,2*]

[1]Department of Chemistry, Faculty of Science, Universiti Putra Malaysia, 43400 UPM, Serdang, Selangor, Malaysia

[2]Natural Medicines and Products Research Laboratory, Institute of Bioscience, Universiti Putra Malaysia, 43400 UPM Serdang, Selangor, Malaysia

[3]Department of Biological Sciences and Biotechnology, Faculty of Science & Technology, Universiti Kebangsaan Malaysia, Bangi, 43600, Selangor, Malaysia

[4]Centre of Foundation Studies for Agricultural Science, Universiti Putra Malaysia, 43400 UPM, Serdang, Selangor, Malaysia
*Correspondence: Siti Munirah Mohd Faudzi**;** sitimunirah@upm.edu.my

Edited by Mohamad Shazeli Che Zain, PhD

Keywords:

Acetophenone
RSM
Anti-tyrosinase
Depigmentation
Zebrafish

Abbreviations:
Box-Behnken design (BBD)
Central Composite Design (CCD)
1-phenyl-2-thiourea (PTU)
Response Surface Methodology (RSM)

ABSTRACT

Hyperpigmentation is characterized by excessive melanin production, often associated with skin irritation and inflammation, leading to uneven skin tone. This underscores the need for safer and more effective depigmenting agents. In this study, the benzoic acid derivative, 4-hydroxyacetophenone (**2**), was synthesized by demethylation of 4-methoxyacetophenone (**1**) using a long-chain thiol. For the first time, this demethylation reaction was optimized using Response Surface Methodology (RSM), offering an efficient approach for hydroxylated compound synthesis. The optimized conditions, 128.85°C, 4.00 mmol 1-dodecanethiol, and 20.752 minutes reaction time, resulted in maximum product yield. Subsequent evaluations demonstrated that minimal acute toxicity was observed at tested concentrations. Depigmentation studies showed significant effects of both compounds **1** and **2** compared to the control group in the zebrafish model. This is the first report demonstrating the depigmenting effect of compound **2** in an in vivo zebrafish model, which is further supported by the tyrosinase inhibitory properties of the compound with an IC_{50} value of 62.72 ± 1.39 µM. Molecular docking confirmed the stronger binding affinity of compound **2** to tyrosinase, showing stronger binding than compound **1** and comparable to the standard control, 1-phenyl-2-thiourea (PTU). Overall, this work highlights the effectiveness of RSM optimization and the potential of hydroxylated acetophenones as anti-tyrosinase agents.

MALAYSIAN NATURAL PRODUCTS SOCIETY

GRAPHICAL ABSTRACT

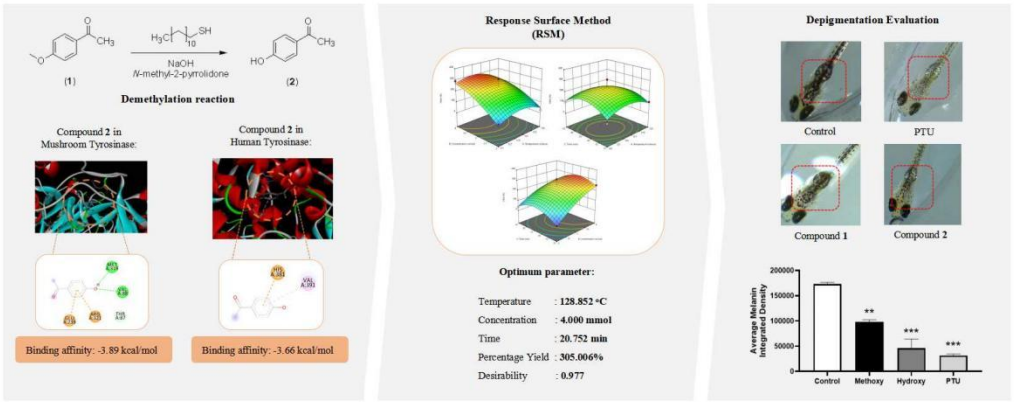

1. INTRODUCTION

Hyperpigmentation is a common dermatological condition in which some areas of the skin are darker than the actual skin colour. Causes of hyperpigmentation include exposure to UV radiation from sunlight, hormonal changes, and skin inflammation. Hyperpigmentation can also affect quality of life and self-image and ultimately lead to psychological problems in patients [1]. Skin pigmentation results from the synthesis of melanin in specialized cells through a process called melanogenesis and the subsequent uniform distribution of this melanin in the keratinocytes of the epidermis. Melanogenesis is the physiological process of melanin formation initiated by tyrosinase, a copper-dependent enzyme [2]. Due to the essential role of tyrosinase in melanogenesis, inhibiting its activity is a useful approach to reduce the overproduction of pigment. Therefore, specific tyrosinase inactivators and reversible inhibitors are needed that effectively bind to the binding pocket of tyrosinase and thus inhibit tyrosinase activity.

Among the tyrosinase inhibitors, hydroquinone is a traditional bleaching agent commonly used in clinical practice. Despite its good efficacy, prolonged use of hydroquinone is associated with side effects such as irritation, inflammation, and an increased risk of cancer [3]. Given the occurrence of side effects with existing anti-tyrosinase agents, continuous efforts have been made to identify alternative tyrosinase inhibitors with high efficacy and low toxicity. Various phenolic derivatives, including thymol, vanillin, and coumarin analogues, have been designed and developed to mimic the natural substrates of the tyrosinase enzyme, the amino acid *L*-tyrosinase [4] and hydroquinone. In addition, compounds such as benzoic acid and cinnamic acid analogues have consistently shown excellent body depigmentation with a better safety profile [5]. Previous studies have established structure-activity relationships (SARs) that emphasize the importance of hydroxyl functions in enhancing tyrosinase inhibition. In addition, the ketone moiety is considered a key structural feature that facilitates strong interactions with the catalytic pocket of tyrosinase, primarily through the hydrogen bond formations [4]. Building on these findings, benzoic acid derivatives, particularly 4-hydroxyacetophenone (**2**), were selected as a case study to further validate and demonstrate their depigmenting potential using the zebrafish in vivo model. This in vivo evaluation serves to complement the existing physicochemical, structural, and molecular docking data to gain a more comprehensive understanding of the compound's efficacy and safety as a potential depigmenting agent.

Based on previous research, compound **2** was commonly synthesized by a demethylation reaction. However, conventional methods for the synthesis of hydroxyl-containing compounds often result in undesirable by-products that compromise yield and purity. As an alternative, the demethylation of 4-methoxyacetophenone (**1**)

to produce compound **2** was performed using a long-chain thiol-mediated strategy (Figure 1). Less-odorous C12 alkanethiols were selected due to their high boiling points, which allow them to withstand the elevated reaction temperature of 130°C[10]. Among these, 1-dodecanthiol was chosen for said favorable physicochemical properties which help minimize side reactions and facilitate cleaner product isolation. Moreover, its commercial availability in large quantities at low cost makes it an attractive reagent for scalable synthesis. To optimize the efficiency of this approach, the reaction parameters (temperature, time, and reactant concentration) were systematically optimized using Response Surface Methodology (RSM). To our knowledge, this is the first study in which RSM has been applied to optimize a thiol-mediated demethylation reaction and serves as a pioneering framework for similar transformations in future synthetic studies. Subsequently, the synthesized compounds were evaluated for their potential anti-tyrosinase activity through in vitro tyrosinase enzymatic assays and an in vivo depigmentation model using zebrafish embryos. Furthermore, molecular docking studies were conducted using AutoDock4 to investigate the binding interactions of compounds **1** and **2** with both mushroom and human tyrosinase enzymes (PDB ID: 2Y9X and 5M8S, respectively). These in silico analyses complement the experimental findings and provide additional insights into the molecular basis of tyrosinase inhibition by the tested compounds.

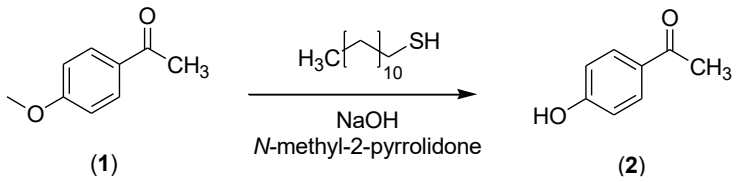

Figure 1 The synthetic preparation of 4-hydroxyacetophenone (**2**) by the demethylation reaction of 4-methoxyacetophenone (**1**)

2. METHODOLOGY

2.1 Chemistry

The solvents and reagents were purchased from R&M Chemicals, Aldrich, Systerm and Alfa Aesar. These chemicals and reagents were used directly for the synthesis without purification. NMR spectra were recorded using a 500 MHz nuclear magnetic resonance (NMR) spectrometer (Varian Inova 500, Illinois, USA) with $CDCl_3$ as solvent, while TMS was used as an internal standard. Chemical shifts and coupling constants are presented in δ (ppm) and *J* (Hz), respectively. The Perkin Elmer RX1 (Massachusetts, USA) was used to obtain Fourier transform infrared (FT-IR) spectra in the mid-IR range (400-4000 cm^{-1}) using the Attenuated Total Reflected (ATR) technique. The direct injection mass spectrometry (DI-MS) spectra were obtained directly with a Shimadzu QP2010-Plus (Kyoto, Japan) without prior separation by liquid chromatography.

2.1.1 Demethylation reaction

A demethylation reaction was performed with 4-methoxyacetophenone (**1**; 2.0 mmol) and sodium hydroxide (NaOH, 6.0 mmol) as the basic catalyst. The reactants were mixed in a resealable reaction tube and purged with inert nitrogen gas. Subsequently, 2 mL of anhydrous *N*-methyl-2-pyrrolidone (NMP) and 1-dodecanethiol were added to the resultant mixture. The reaction was stirred under controlled temperature and time, as set by the experimental trials guided by the RSM, which are discussed in detail in a subsequent section. Upon completion, thin-layer chromatography (TLC) analysis was carried out to monitor the formation of the demethylated product, compound **2**. The reaction mixture was then cooled to room temperature, acidified with HCl, and extracted with ethyl acetate. The aqueous phase was extracted twice with ethyl acetate (2 x 15 mL), and the combined organic layers were washed with water and brine, dried over anhydrous Na_2SO_4, and concentrated in vacuo. The crude

product was purified and subjected to ^{1}H NMR ($CDCl_3$ as solvent), FT-IR, and DI-MS analyses to confirm the identity, purity, and structural integrity of the demethylated compound produced.

4-methoxyacetophenone **(1)**

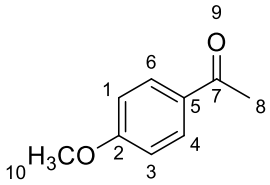

White powder and melting point: 36 - 40°C. ^{1}H NMR (500MHz, $CDCl_3$) exhibited signals at δ 2.53 (s, 3H, H-8), 3.85 (s, 3H, H-10), 6.91 (d, *J*=7.04 Hz, 2H, H-4 and H-6), and 7.92 (d, *J*=7.04, 2H, H-1 and H-3).

4-hydroxyacetophenone **(2)**

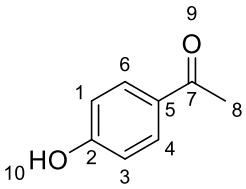

White solid, yield 48.03% and melting point: 106 - 108°C. ^{1}H NMR (500MHz, $CDCl_3$) exhibited signals at δ 2.55 (s, 3H, H-8), 6.87 (d, *J*=7.12 Hz, 2H, H-4 and H-6), and 7.90 (d, *J*=7.16, 2H, H-1 and H-3). MS m/z 402.00 (3[M]$^+$, $C_8H_8O_2$, calculated 136.00).

2.1.2 Optimization of demethylation reaction

The optimization of demethylation reaction conditions was performed using RSM. RSM is an effective statistical approach to establish the relationship between the process variables and the desired response. A face-eCentral Composite Design (CCD) was initially selected to investigate three critical factors: 1-dodecanethiol concentration (2-4 mmol), temperature (125-135°C), and time (10-35 min) [6]. The objective was to identify the optimal conditions for maximizing the product yield (the response variable). Subsequently, a Box-Behnken design (BBD) was applied using Design Expert version 13.0 (Stat-Ease Inc., Minneapolis, USA), which requires three levels (-1, 0, 1) for each variable and allows systematic evaluation of the main, interaction, and quadratic effects of the factors [6], as tabulated in Table 1. The selected parameters and their levels are detailed in Table 1, and the experimental design matrix is shown in Table 2. An analysis of variance (ANOVA) was also performed to assess the statistical significance and adequacy of the constructed model. The coefficient of determination (R^2) was used to assess the predictive power of the model and to explain the variability of the optimization parameters, which is a measure of the percentage of variance explained by the model. In addition, three-dimensional (3D) response surface graphs were generated to visualize the relationship between the variables and subsequently determine the optimal response conditions.

Table 1 Parameter input and its levels in RSM

Parameters	**Coded levels**		
	-1	**0**	**+1**
Concentration 1-dodecanethiol (mmol)	2.0	3.0	4.0

Temperature (°C)	125	130	135
Time (min)	10.0	22.5	35.0

Table 2 Experimental trials with selected parameters (the concentration of 1-dodecanethiol, temperature, and time) in RSM

Run	A: Temperature (°C)	B: Concentration (mmol)	C: Time (min)
1	135	3	10.0
2	135	2	22.5
3	125	3	35.0
4	130	4	35.0
5	130	4	10
6	130	3	22.5
7	125	2	22.5
8	130	3	22.5
9	135	4	22.5
10	130	3	22.5
11	130	3	22.5
12	130	2	10
13	130	3	22.5
14	125	4	22.5
15	135	3	35
16	125	3	10
17	130	2	35

2.2 Biology

2.2.1 Animal husbandry

All experiments with wild-type (WT) zebrafish were approved by the Institutional Animal Care and Use Committee (IACUC) of the Animal Ethics Committee of Universiti Putra Malaysia (IACUC-R024/2023). Adult zebrafish (WT strains), all older than 6 months, were maintained in 2-L aquaria at 25–27ºC with a 10:14 hour dark-light cycle. The fish were maintained in a ratio of 2 males to 3 females in a single tank to create a stress-free environment for breeding. The WT fish were fed brine shrimp (Artemia, Super Artemia (M) Sdn Bhd, Shah Alam, Selangor, Malaysia) 3 to 4 times per day, alternating with commercial flake food (Ziegler, Gardners, USA). A constant recirculation pump was used to maintain the water system in the aquarium.

2.2.2 Experimental conditions and chemical exposure

Zebrafish embryos were exposed to acetophenones (**1** and **2**), with 1-phenyl-2-thiourea (PTU) as a positive control. The concentration range for the acetophenones was determined by twofold serial dilution, starting at 200 µM down to 7.25 µM. For PTU, only two concentrations (200 µM and 100 µM) were used as these concentrations have been commonly used in previous studies to inhibit pigmentation in zebrafish embryos with minimal side effects [7]. Chemical exposure to all three compounds was initiated 5 hours post-fertilization (hpf) of the embryos. Each treatment was tested at six different concentrations with three replicates per concentration. For each replicate, 10 embryos were placed in individual wells of a 24-well plate (n = 30 embryos per treatment group).

2.2.3 Zebrafish embryo toxicity assay

A series of toxicity assessments were conducted to determine the safe and non-toxic concentrations of compound **1**, compound **2**, and PTU tested. These assessments included spontaneous tail coiling (STC), heart rate, hatch rate, and survival rate, which collectively serve as early indicators of neurotoxicity, cardiotoxicity, developmental toxicity, and overall viability. At 24 hpf, embryos were acclimatized for one minute, and STC was assessed by manually counting the number of tail coiling movements over one minute. A complete coil was defined as a lateral movement of the embryo's trunk from side to side. Abnormal STC patterns, i.e., either reduced or excessive coiling frequency, may indicate potential neurotoxicity. This test is usually performed between 6 and 24 hpf, which coincides with early neurodevelopment [8]. Cardiotoxicity was assessed at 48 hpf by measuring heart rate, expressed in beats per minute (bpm), under a stereomicroscope. After 72 hpf, the hatching rate was recorded to assess potential developmental toxicity. It was calculated as the percentage of embryos successfully hatched from their chorions relative to the total number of embryos incubated. Survival was also recorded daily throughout the exposure period to monitor the overall viability of the embryos. All analyses were performed using a stereomicroscope (Leica EZ4W, Leica Microsystems; Wetzlar, Germany).

2.2.4 Depigmentation effect on zebrafish

Chemical exposure was extended up to 5 days post-fertilization (dpf). During this time, zebrafish larvae treated with acetophenones (**1** and **2**) and PTU were carefully monitored. The effects of depigmentation were assessed by observing the larvae under a Leica EZ4W stereomicroscope. To quantitatively assess the pigment changes, the integrated melanin density within a defined region of interest (ROI) was measured in each larvae. High-resolution images of the larvae were captured and subsequently analyzed using ImageJ software (National Institutes of Health, Maryland, USA). The ROI was selected based on areas commonly used for pigmentation analysis, such as the dorsal head and trunk area. The measured integrated density values provided a quantitative representation of melanin content and allowed comparison between the treated groups and the untreated control.

2.2.5 Mushroom tyrosinase enzymatic assay

Following the evaluation of depigmentation in zebrafish, an in vitro mushroom tyrosinase inhibition assay was conducted to evaluate the ability of acetophenones (**1** and **2**) to inhibit tyrosinase activity. This assay is crucial to complement the in vivo results, as melanogenesis can be mediated by inhibition of the tyrosinase mechanism, a key enzyme in melanin biosynthesis. The experiment was performed based on the method described by Zakaria et. al. (2021), with minor modifications [9]. The assay was conducted in 96-well microplates in which 100 µL of the test samples were filled and serially diluted to obtain final concentrations between 200 and 3.13 µM. Subsequently, 40 µL of the mushroom tyrosinase enzyme solution (333 U/mL) was added to each well. A similar

volume of phosphate buffer solution was used for the blank wells. Dimethyl sulfoxide (DMSO, 0.4%) was used as a negative control, while kojic acid was used as a positive control for comparison. After a pre-incubation period of 5 minutes at 25°C, 40 µL of L-DOPA substrate (2.5 mM) was added to initiate the reaction. The test mixtures were then incubated for a further 15 minutes at room temperature. The absorbance was measured at 450 nm using a microplate reader (Tecan Safire, Grödig, Austria). All samples were tested in triplicate, and the percentage of tyrosinase inhibition was calculated using Equation 1.

$$\text{Tyrosinase inhibition activity (\%)} = \frac{Absorbance\ control - Absorbance\ sample}{Absorbance\ control} \text{x } 100\% \quad (1)$$

2.2.6 Statistical analysis

All data were expressed as mean ± standard error of the mean (SEM) and analyzed using GraphPad Prism version 9.3.0 (GraphPad Software, San Diego, CA, USA). Prior to statistical analysis, the data were subjected to a normality test. A one-way analysis of variance (ANOVA) was then performed to assess differences in toxicity parameters and integrated melanin density between treatment groups. Where significant differences were found, Tukey's post hoc test for multiple comparisons was applied. A p-value of ≤ 0.05 was considered statistically significant.

2.3 Computational chemistry: Molecular docking

Molecular docking simulations were performed to predict the binding interactions of the selected compounds with two tyrosinase enzymes: mushroom tyrosinase from Agaricus bisporus (PDB ID: 2Y9X) and human tyrosinase in complex with PTU (PDB ID: 5M8S). Tropolone was used to validate the docking parameters for the mushroom tyrosinase, while PTU was used for the human tyrosinase. Docking simulations were carried out using AutoDock Tools version 4.2.6 (The Scripps Research Institute, La Jolla, CA, USA). The protein structures were prepared by: (1) removing native ligands, water molecules, small molecules, and unwanted residues with Discovery Studio Visualizer v19.1.0.18287; (2) adding all missing hydrogen atoms; (3) assigning the charges of the combined Kollman atoms; and (4) saving the files in .pdbqt format. The two-dimensional structures of the acetophenone derivatives were generated from PubChem SMILES notations (CIDs: 7476 and 7469) and converted to PDB format using Avogadro version 1.2.0. The ligand structures were further prepared in AutoDock Tools 1.5.6 and saved as .pdbqt files. For the mushroom tyrosinase, the size of the grid box was set to 30 × 30 × 30 Å with a spacing of 1,000 Å, centered on the coordinates X: -10.215, Y: -28.653, Z: -43.443. For human tyrosinase, the grid box was 24 × 24 × 24 Å with a spacing of 1,000 Å, centered at X: 121.02, Y: 135.285, Z: 217.141. In both cases, the grid box was centered on the active site containing two metal ions.

3 RESULTS AND DISCUSSION

3.1 Chemistry

3.1.1 Optimization of demethylation reaction

In the synthesis, 4-methoxyacetophenone (**1**) was used as a model substrate for the demethylation process to yield 4-hydroxyacetophenone (**2**), using 1-dodecanethiol, as a mediator instead of conventional demethylation reagents, as shown in Figure 2. This approach has been shown to provide a clean and efficient conversion to the desired phenolic compound for a wide range of substrates [10]. The optimal conditions for the demethylation reaction were determined using RSM. The highest yield of compound **2** based on the BBD is summarized in Table

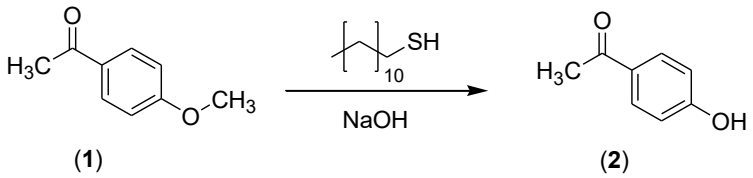

Figure 2 Mechanism of formation of 4-hydroxyacetophenone (**2**) by the demethylation reaction

With regard to the optimization target, Table 3 shows that run 14 produced the highest predicted response value (289.41, scaled %). This result indicates a generally good agreement between the experimental (actual) values and the values predicted by the model and thus confirms the reliability of the RSM. The immediate yield was used instead of purified yield to avoid potential loss of compound **2** during purification, as inconsistent recovery could compromise the validity of the RSM model. Minor deviations from the predicted values can be attributed to experimental factors, such as slight variations in temperature control or mixing efficiency during the reaction process. Furthermore, a second-order polynomial regression equation (Equation 2) was developed to represent the relationship between the independent variables and the percentage yield of the desired product. This predictive model serves as a useful tool for estimating product yield under different experimental conditions and as a guide for future reaction optimization efforts.

$$\text{Yield} = 238.59 - 12.63A + 97.59B - 3.68C - 17.35AB - 12.1AC - 22.17BC - 61.57A - 36.43B^2 - 82.42C^2 \quad (2)$$

Where A, B, and C represent the values of temperature, the concentration of 1-dodecanethiol, and time, respectively.

Table 3 Actual and predicted value of percentage yield of the 4-hydroxyacetophenone (compound **2**) based on the varied set of reaction parameters using RSM

Run	A: Temperature (°C)	B: Concentration (mmol)	C: Time (min)	Yield of compound 2 (%)	
				Actual	Predicted
1	135	3	10	107.94	97.74
2	135	2	22.5	26.47	47.72
3	125	3	35	105.44	115.64
4	130	4	35	180.44	191.49
5	130	4	10	253.09	243.18
6	130	3	22.5	221.91	238.59
7	125	2	22.5	58.38	38.27
8	130	3	22.5	311.91	238.59
9	135	4	22.5	188.09	208.20
10	130	3	22.5	232.94	238.59
11	130	3	22.5	218.68	238.59
12	130	2	10	14.7	3.65

13	130	3	22.5	207.5	238.59
14	*125*	*4*	*22.5*	*289.41*	*268.16*
15	135	3	35	97.35	66.19
16	125	3	10	67.65	98.81
17	130	2	35	30.73	40.64

The ANOVA analysis performed with the Design Expert software confirms the adequacy and suitability of the quadratic response surface model for the description of the experimental data, as summarized in Table 4. This is supported by a high F-value of the model (9.36), a very low P-value ($P < 0.05000$), and a satisfactory R^2, all of which indicate the statistical significance and desirability of the model [11]. The significant F-value indicates that the variation in response can be adequately explained by the model terms and not by random error. In addition, the non-significant test for lack of fit (F-value = 0.8137; P = 0.5494) relative to the pure error confirms the appropriateness of the model, as a significant lack of fit would indicate that the model does not adequately capture the experimental variability. Therefore, the statistical results confirm that the quadratic model is robust and reliable for predicting the percentage yield of compound **2** under the reaction conditions investigated [12]. Figure 3 further illustrates the comparison of the predicted (linear graph) and actual values for each run.

Table 4 ANOVA results in the quadratic reaction surface model of the percentage yield of 4-hydroxyacetophenone (**2**) for the effect of all independent variables

Source	Sum of Squares	df	Mean Square	F-value	P-value	
Model	1.37E+05	9	15182.26	9.36	0.0038	**Significant**
A-Temperature	1275.88	1	1275.88	0.7868	0.4045	
B-Concentration	76196.32	1	76196.32	46.99	0.0002	
C-Time	108.19	1	108.19	0.0667	0.8036	
AB	1204.44	1	1204.44	0.7428	0.4173	
AC	585.16	1	585.16	0.3609	0.567	
BC	1966.04	1	1966.04	1.21	0.3073	
A^2	15962.96	1	15962.96	9.84	0.0164	
B^2	5587.29	1	5587.29	3.45	0.1058	
C^2	28602.52	1	28602.52	17.64	0.004	
Residual	11350.66	7	1621.52			**Not significant**
Lack of Fit	4301.7	3	1433.9	0.8137	0.5494	
Pure Error	7048.96	4	1762.24			
Cor Total	1.48E+05	16				

A further validation of the model was carried out. The results are presented in Figure 3, which shows a comparison between the predicted and experimental percentage yields in relation to all three independent variables. The corresponding values of the regression coefficients for the final reduced model are summarized in Table 5. The R^2 was found to be 0.9233, indicating that approximately 92.33% of the variability in the percentage yield can be explained by the model. The adjusted R^2 value of 0.8247 emphasizes the accuracy of the model, considering the number of predictors included in the model. In addition, the adequate precision value reflecting the signal-to-noise ratio was calculated to be 8.5645. As this value exceeds the minimum acceptable threshold of 4, it confirms that the model has an adequate signal and can be reliably used for exploration and navigation in the design space [13]. Overall, these statistical parameters validate the robustness and predictive ability of the model. To further improve the reliability and reproducibility of the results, it is recommended to repeat certain experimental runs at least three times to minimize variability and ensure the accuracy of the percentage yield data.

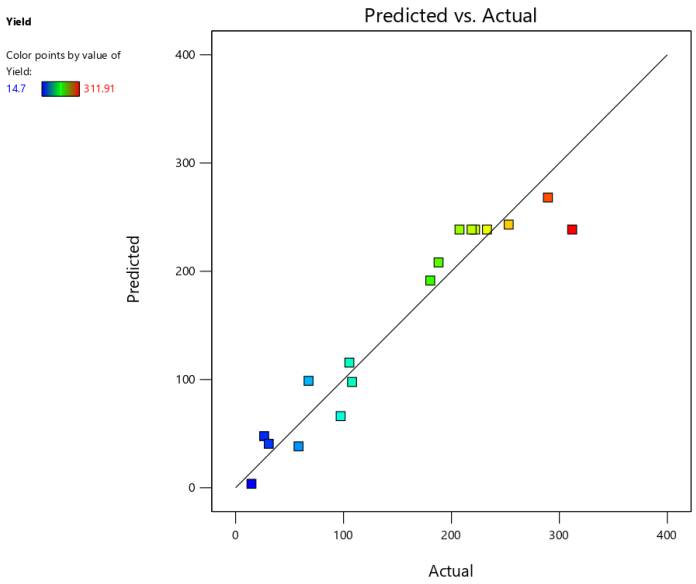

Figure 3 The comparison graph of the predicted and actual values of the percentage yield of 4-hydroxyacetophenone (**2**) based on three variables

Table 5 Statistical analysis of the quadratic mode for the final reduced model

Std. Dev.	40.27	**R^2**	0.9233
Mean	153.68	**Adjusted R^2**	0.8247
C.V. %	26.2	**Predicted R^2**	0.4605
		Adeq Precision	8.5645

Received: 23/7/2025 | Accepted: 17/9/2025 | Published: 30/1/2026

3.1.2 Response surface analysis

Optimizing reaction conditions is a critical step in maximizing product yield and increasing the overall efficiency of chemical synthesis. Although this process can be time-consuming, it is important to systematically consider various influencing factors such as temperature, reagent concentration, and reaction time to ensure optimal reaction performance. In this study, the demethylation of 4-methoxyacetophenone (**1**) to 4-hydroxyacetophenone (**2**) using 1-dodecanethiol as a nucleophilic reagent had to be carefully optimized to achieve a high yield of the target product. Accordingly, the demethylation reaction was optimized by varying three independent variables: reaction temperature, 1-dodecanethiol concentration, and reaction time. The influence of these variables on the percentage yield was evaluated using RSM, and the results were visualized by 3D surface plots generated using Design-Expert® software (Stat-Ease Inc., Minneapolis, MN, USA).

Figure 4a shows the interactive effect of reaction temperature and 1-dodecanethiol concentration on the percentage yield of compound **2**. The results indicate that the yield increases as the concentration of 1-dodecanethiol increases from 2 mmol to 4 mmol. This observation is consistent with previous findings [10] where 1-dodecanethiol acts as a nucleophile in the substitution mechanism (as illustrated in Figure 2). Higher concentrations of the nucleophile promote the substitution reactions and thus product formation. However, the yield also depends strongly on the temperature. While a moderate increase in temperature generally accelerates the substitution reactions (S_N2), too high temperatures can promote competing elimination reactions and thus reduce the efficiency of product formation. Therefore, identifying an optimal temperature range, especially between 125°C and 135°C, is crucial for maximizing yield. Figure 4b illustrates the combined effect of reaction temperature and time on product yield. In line with the previous trend, the optimum yield is achieved at an average reaction time of 10 to 35 minutes. Previous studies [10] have shown that the conversion of methoxy-containing compounds to hydroxylated products is rapid, especially in the presence of electron-withdrawing groups. Although shorter reaction times may be sufficient for the initial conversion, extending the reaction time ensures maximum substrate utilization and improves the overall yield. Figure 4c depicts the interaction between 1-dodecanethiol concentration and reaction time. The plot indicates that higher yields are achieved when the concentration of the demethylating agent is high and the reaction time is moderate. This emphasizes the importance of a balanced ratio between reagent concentration and reaction time to achieve optimal demethylation efficiency. To summarize, the response surface analysis confirms that the yield of 4-hydroxyacetophenone (**2**) is significantly influenced by the interplay of temperature, reagent concentration, and reaction time. Careful adjustment of these parameters is essential to ensure successful and efficient demethylation under mild and practical reaction conditions.

(**a**) (**b**) (**c**)

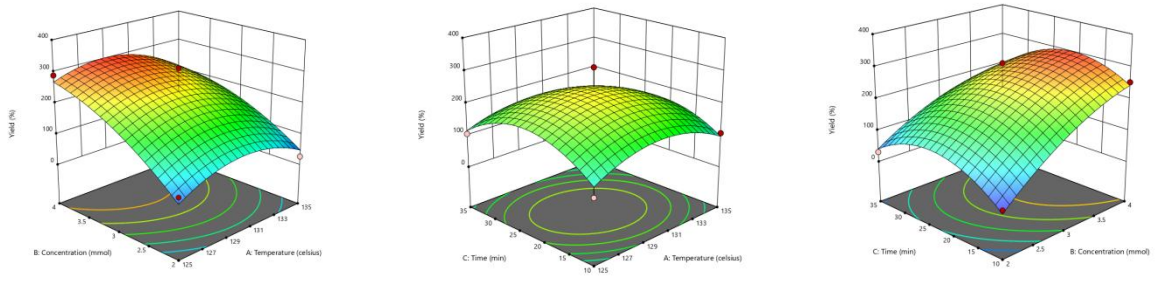

Figure 4 Three-dimensional response surface showing the effect of (**a**) 1-dodecanethiol concentration and temperature; (**b**) temperature and reaction time; (**c**) 1-dodecanethiol concentration and reaction time

3.1.3 Verification of model

To validate the accuracy and reliability of the predicted response values, the final mathematical model was subjected to a verification process. The adequacy of the model was assessed by generating several randomized formulations near the predicted optimal conditions. For each formulation, the corresponding point predictions were determined using Design-Expert® software (Stat-Ease Inc., Minneapolis, Minnesota, USA). Table 6 shows a comparative analysis of the actual versus predicted percentage yields of compound **2**. To quantitatively evaluate the deviation between the experimental and predicted values, the relative standard error (RSE) was calculated using Equation 3. The validation procedure comprises three different test series, and the corresponding RSE values are summarized in Table 6. It is generally recognized that an RSE value below 5 % indicates a high degree of model accuracy and reliability [14]. The results show that all three-test series yielded RSE values within the acceptable threshold, confirming the robustness and predictive ability of the developed model. These results validate that the proposed model can be reliably used to predict the percentage yield under optimized reaction conditions.

$$\text{RSE (\%)} = \left| \frac{\text{Actual value} - \text{Predicted value}}{\text{Predicted value}} \right| \times 100\% \quad (3)$$

Table 6 Predicted and actual response value for the random percentage yield of 4-hydroxyacetophenone (**2**) via the optimized demethylation reaction.

Set	Independent Variables			Response Variables		RSE (%)
	A: Temperature	B: Concentration	C: Time	Actual	Predicted	
1	125	3.75	20	247.00	253.708	2.64
2	130	3.5	20.5	292.40	278.53	4.98
3	130	3.75	21	278.88	272.542	2.33

3.1.4 Optimization of response

The Design-Expert® software was used to optimize the reaction parameters for the demethylation process. The aim of the optimization was to determine the most effective combination of all three independent variables, reaction temperature, concentration of 1-dodecanethiol, and reaction time, within the specified ranges to maximize the percentage yield of compound **2**. The numerical optimization process was performed using the software's built-in optimization algorithm, which considers both the individual and interactive effects of the variables on the response. The optimization results, including the proposed optimal conditions, are shown in Table 7. The optimized conditions for the demethylation reaction derived using the BBD-RSM recommended a reaction temperature of 128.85°C, a 1-dodecanethiol concentration of 4.00 mmol, and a reaction time of 20.75 min. These conditions were associated with a high desirability value of 0.977, indicating the robustness and reliability of the optimized model. A summary of the final optimized parameters and the corresponding predicted percentage yield is provided in Table 8, confirming the effectiveness of the RSM-based optimization approach in improving the efficiency of the synthesis process.

Table 7 Constraints of numerical optimization

Name	Goal	Lower Limit	Upper Limit
A: Temperature	is in range	125	135
B: Concentration	is in range	2	4

C: Time	is in range	10	35
Yield	maximize	14.7	311.91

Table 8 Optimum condition for demethylation reaction

Independent Variable			Percentage Yield (%)	Desirability
Temperature (°C)	Concentration of 1-dodecanthiol (mmol)	Reaction Time (min)		
128.850	4.000	20.754	305.006	0.977

3.1.5 Structural characterization

The structural characterization of the synthesized compound **2** was carried out by comparing the ^{1}H NMR spectra of the starting material (**1**) and the product. In compound **1**, the methoxy group (-OCH_3) is observed as a strong singlet peak at δ = 3.85 ppm (Supplementary Figure S1). After successful demethylation, this peak disappears in the spectrum of compound **2**, and a small broad singlet peak appears in the range of δ = 3.00–4.50 ppm, indicating the presence of a hydroxyl proton (Supplementary Figure S2). A comparative summary of the NMR data is provided in Supplementary Table S1. Further confirmation was obtained by FT-IR analysis, where the spectrum of compound **2** showed a broad absorption band at 3447.44 cm^{-1} corresponding to the O–H stretching vibrations, further verifying the successful demethylation compared to compound **1** (Supplementary Figure S3). Moreover, DI-MS analysis of compound **2** revealed a molecular ion peak at m/z 136, consistent with the molecular formula $C_8H_8O_2$ (Supplementary Figure S4). The observed ion was attributed to a trimeric form $[3M]^+$. Fragmentation patterns further supported the compound's identity, with characteristic fragment ions detected at m/z 103, 96, and 43. These data are summarized in Supplementary Table S2, and the proposed fragmentation mechanism is illustrated in Supplementary Figure S5. Subsequently, 4-methoxyacetophenone (**1**) and the purified product, 4-hydroxyacetophenone (**2**), were subjected to in vivo toxicity profiling and depigmentation evaluation using the zebrafish model.

3.2 Biology

3.2.1 Toxicity evaluation using in vivo model

Toxicity profiling is the first and essential step to determine the safe and effective concentration range of test compounds prior to evaluating their potential depigmentation effects. In this study, four different toxicity endpoints were assessed in zebrafish embryos exposed to acetophenones: STC rate, heartbeat rate, hatching rate, and survival rate. Each assay was performed in triplicate to ensure the reliability and reproducibility of the data.

STC, an early motor behaviour of the embryo, is often used as an indicator of developmental neurotoxicity [15]. STC was first observed at 24 hpf. As shown in Figure 5a, no significant differences in STC rate were observed in embryos exposed to either compound **1** or compound **2**, except at 25 µM of compound **2**, where a significant reduction in STC rate was observed. This result could indicate possible acute neurotoxicity at higher concentrations of compound **2**. However, further studies are needed to validate this result and clarify the underlying mechanisms. In addition to the neurodevelopmental endpoints, a cardiovascular assessment was performed by monitoring the heart rate of the embryos. The normal heart rate of zebrafish embryos is between 120–180 beats per minute (bpm) [16]. As shown in Figure 5b, embryos exposed to 25 µM of compound **1**

exhibited a significantly increased heart rate compared to both the control and the same concentration of compound **2**.

In contrast, compound **2** did not cause significant changes in heart rate at all concentrations tested. These results suggest compound **1** may cause mild cardiotoxic effects at higher concentrations and warrant further investigation. At 72 hpf, hatching rate was evaluated as a marker of normal embryonic development, as hatching signifies the successful transition from embryo to larva [17]. No significant differences in hatching rates were observed in all treatment groups, indicating that neither compound had a negative effect on development at the concentrations tested (Figure 5c). Finally, survival was evaluated up to 3 dpf to assess overall embryotoxicity. As can be seen in Figure 5d, both compounds exhibited no significant differences in survival compared to the control group during the 72-hour exposure period. In summary, both compounds **1** and **2** showed minimal acute toxicity in zebrafish embryos at the concentrations tested. These results support the use of these compounds at lower concentrations in subsequent depigmentation studies.

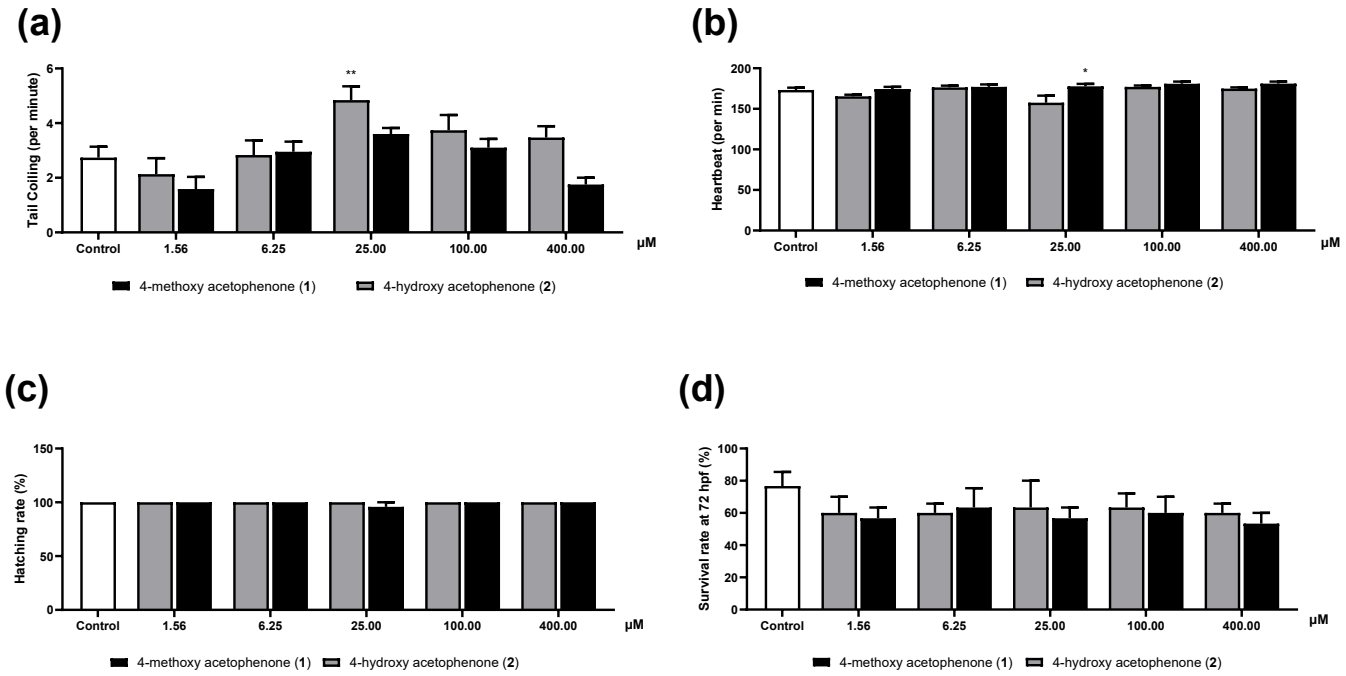

Figure 5 Toxicity profiles of zebrafish embryos were assessed at 24 to 72 hpf after exposure to acetophenones (compounds **1** and **2**), based on: (**a**) spontaneous tail coiling, (**b**) heart rate, (**c**) hatching rate, and (**d**) survival rate. Statistical analysis was performed using the one-way ANOVA test followed by a Tukey post-test (*$p < 0.05$, **$p < 0.01$)

3.2.2 Depigmentation effect

The zebrafish in vivo model is a valuable tool for assessing the depigmentation potential and toxicity profile of test compounds, including their effects on developmental mortality and malformations. This suitability is due to the high degree of genetic and physiological similarity between zebrafish and humans, particularly in gene expression and regulatory pathways involved in melanocyte differentiation and proliferation. As a result, the development of melanocytes in zebrafish parallels that of humans with only minor differences [18].

The process of eumelanin synthesis in zebrafish mirrors that of mammals and involves three important melanogenic enzymes: tyrosinase (TYR), tyrosinase-related protein-1 (*trp-1*), and tyrosinase-related protein-2 (*trp-2*). These enzymes contribute to melanin production, which is subsequently stored in specialized organelles

called melanosomes within melanocytes [19]. In this study, PTU, a well-established tyrosinase inhibitor, was used as a positive control. As reported by [7], a concentration of 0.003% PTU effectively inhibits pigmentation and maintains embryo transparency during early zebrafish development, demonstrating its potent depigmenting effect despite known side effects that limit its suitability for human use. The efficacy of PTU is visually evident in Figure 6a, which shows a marked reduction in pigmentation in PTU-treated embryos compared to untreated controls. A depigmenting effect was observed in embryos treated with compound **1** and compound **2** (Figure 6b). Furthermore, the quantitative analysis in Figure 7 further illustrates the average melanin density in all treatment groups. PTU exhibited the lowest melanin density, followed by compound **2** and compound **1**. These results suggest that compound **2** has a stronger depigmenting effect than the methoxylated compound **1**, highlighting the critical role of the hydroxyl group in enhancing target bioactivity.

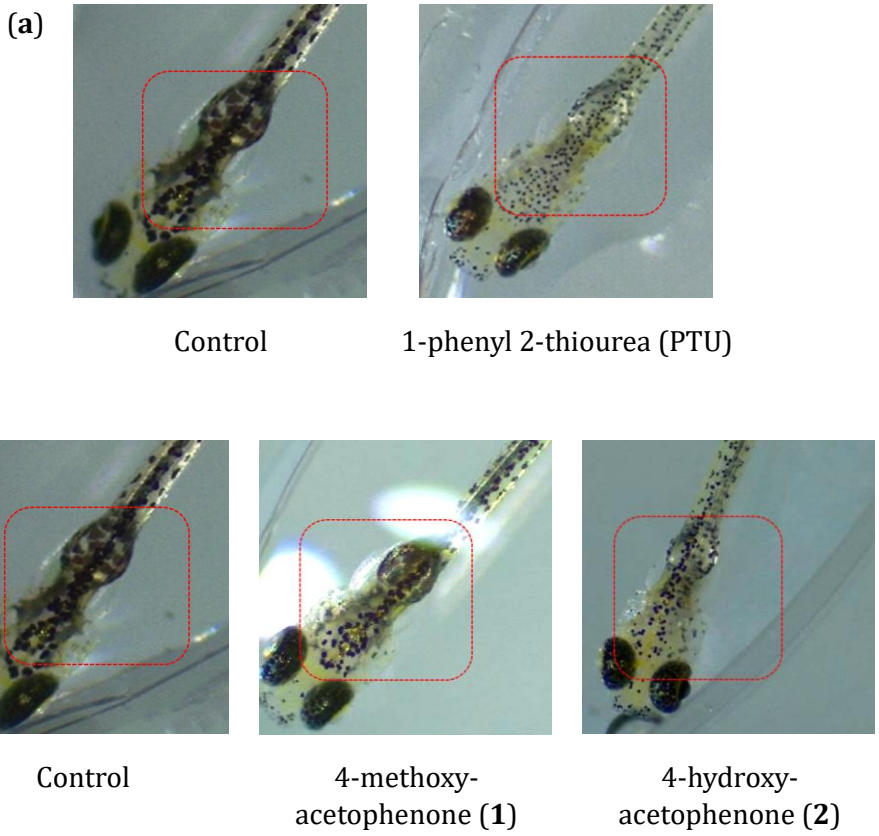

Figure 6 Depigmentation of zebrafish upon exposure to (**a**) PTU and (**b**) 4-methoxyacetophenone (**1**) and 4-hydroxyacetophenone (**2**)

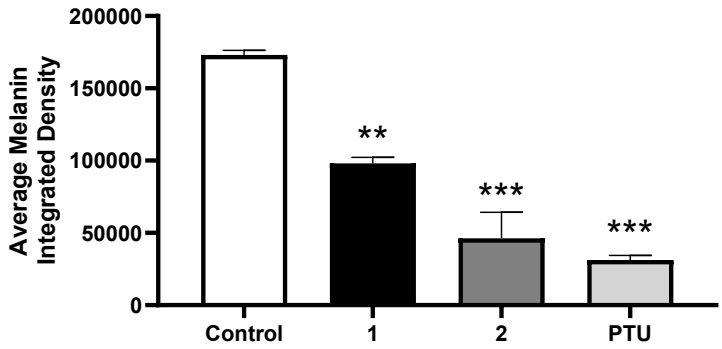

Figure 7 Average integrated melanin density measured in different exposure groups of the zebrafish *in vivo* model

3.2.3 Mushroom tyrosinase enzymatic assay

The mushroom tyrosinase enzymatic in vitro assay is a widely used screening method to evaluate the depigmenting effect of test compounds. Tyrosinase plays a central role in melanin biosynthesis by catalysing the oxidation of L-DOPA to dopaquinone, a key step in the melanin production pathway. Therefore, inhibition of tyrosinase activity is an important indicator of a compound's potential to act as a depigmenting agent. As shown in Table 9 and Supplementary Figure S6, compound **2** demonstrated a lower IC_{50} value compared to compound **1**, indicating a stronger inhibitory effect on tyrosinase activity. Although both compounds were less effective than kojic acid, which served as a positive control, the results clearly suggest that the hydroxyl moiety in compound **2** enhances its inhibitory effect more effectively than the methoxy group in compound **1**.

Importantly, these in vitro results are consistent with the in vivo observations of the zebrafish model (discussed in Section 3.2.1.2), in which compound **2** also showed a stronger depigmenting effect compared to compound **1**. Overall, the complementary evidence from both the in vitro enzyme assays and the in vivo zebrafish experiments strongly supports the superior depigmenting potential of compound **2**. These results emphasize the importance of the hydroxyl functional group in enhancing tyrosinase inhibition and make compound **2** a promising candidate for further development as a depigmenting agent.

Table 9 Tyrosinase activity of acetophenones (compounds **1** and **2**) and kojic acid. The screening and IC_{50} values of the triplicates are expressed as means ± SEM. The different superscript letters represent significant differences at $p < 0.05$ between samples

Compound	Tyrosinase inhibition at 200 µM (%)	IC_{50} ± SEM (µM)
4-methoxyacetophenone (**1**)	55.59	143.10 ± 7.55^{B}
4-hydroxyacetophenone (**2**)	74.23	62.72 ± 1.39^{AB}
Kojic acid	92.12	24.54 ± 4.43^{A}

3.3 Molecular docking

Following the completion of all biological assays, molecular docking studies were performed to elucidate the binding interactions between the acetophenones and two target proteins: mushroom tyrosinase (PDB ID: 2Y9X) and human tyrosinase (PDB ID: 5M8S). The inclusion of molecular docking serves to complement and validate the experimental findings, in particular the in vitro tyrosinase inhibition assay (using 2Y9X) and the in vivo zebrafish depigmentation model (using 5M8S). While the mushroom tyrosinase is an established enzymatic assay platform, the human tyrosinase was chosen to better reflect the physiological relevance of the zebrafish in vivo model, as the genetic and functional similarities between zebrafish and humans are well documented [20]. Therefore, molecular docking to the human tyrosinase provides additional mechanistic insights into the depigmenting effects observed in the zebrafish model.

In the mushroom tyrosinase model (PDB ID: 2Y9X), compound **2** showed the most favourable binding affinity with a binding energy of -3.89 kcal/mol, outperforming compound **1** (-3.67 kcal/mol) and the standard inhibitor PTU (-3.07 kcal/mol). The increased binding affinity of compound **2** is attributed to the *para*-hydroxyl substitution, which facilitates the formation of conventional H-bonds with the key residues VAL88 and MET319. In addition, a C–H bond interaction was observed between the oxygen atom of the hydroxyl group and the THR87 residue, which further stabilizes the ligand–protein complex (Figure 8a). Although the binding affinities (-3.6 to

-3.9kcal/mol) were modest compared to strong inhibitors (≤ -6 kcal/mol), docking alone do not fully predict biological activity. Favorable interactions such as hydrogen bonding and hydrophobic contacts within the active site significantly contribute to meaningful inhibition. Most importantly, both compound **1** and compound **2** outperform the standard inhibitor PTU in silico, suggesting potential for comparable or improved activity in vitro. These findings highlight the central role of the hydroxyl moiety in strengthening molecular interactions within the tyrosinase active site and emphasize its importance in structure-activity relationship (SAR) studies.

A complementary docking analysis against human tyrosinase (PDB ID: 5M8S) further validated the depigmenting potential of compound **2**, which again exhibited the lowest binding energy (-3.66 kcal/mol), followed by compound **1** (-3.37 kcal/mol) and PTU (-3.19 kcal/mol). Although compound **1** had a higher affinity, the ligand–protein interactions were relatively limited compared to the mushroom tyrosinase model. Two important non-covalent interactions were identified between the aromatic ring of compound **2** and the HIS381 residue at the active site: π-cation and π-π stacking (Figure 8b). Interestingly, the hydroxyl group in this model did not form conventional H-bonds, which is likely due to structural differences in the enzyme active site, particularly the presence of two redox-inactive zinc ions in human tyrosinase, which may influence ligand binding orientation and interaction patterns [21]. The binding interaction of compound **2** and PTU in the active site of mushroom and human tyrosinase are listed in Supplementary Tables S3 and S4, respectively.

Taken together, these docking results suggest that although the hydroxyl group contributes significantly to the overall binding affinity in both enzyme systems, its specific role in the interaction mechanisms varies depending on the structural and catalytic architecture of the target protein. These findings underpin the promising inhibitory potential of 4-hydroxyacetophenone (**2**) and provide valuable insights for the future design and development of effective tyrosinase-targeted depigmenting agents. Nevertheless, a moleculer dynamic (MD) study is recommended to complement the docking results, as it provides a dynamic view of molecular interactions and deeper insights into biomolecular behavior, including conformational flexibility and binding energies.

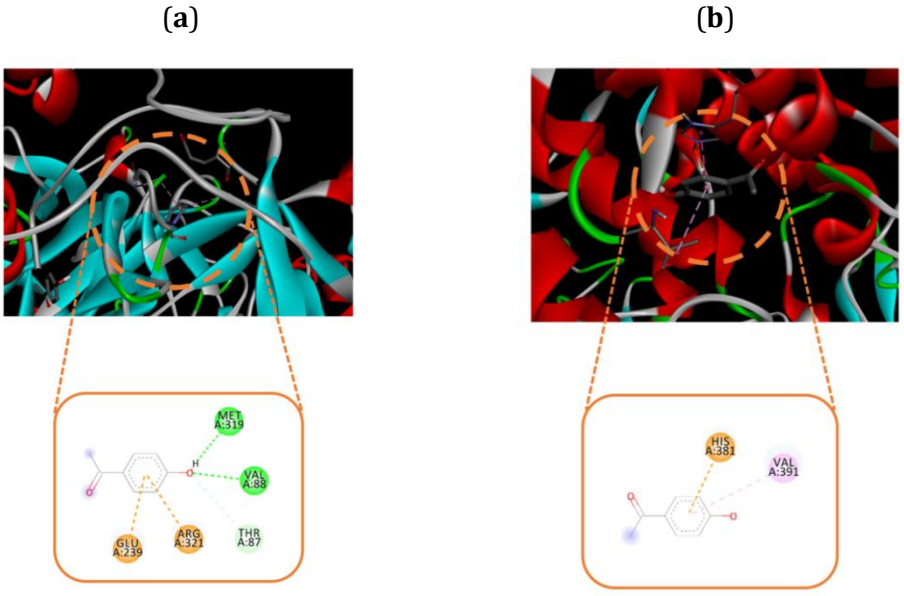

Figure 8 3D and 2D diagram of the binding interactions of 4-hydroxyacetophenone (**2**) in (**a**) mushroom tyrosinase (PDB ID: 2Y9X) and (**b**) human tyrosinase (PDB ID: 5M8S) receptor. (Green line: H-bond; light green line: C-H bond; orange line: π-cation/anion; light purple: π-alkyl)

4 CONCLUSION

In conclusion, this study presents preliminary findings on the development of a potential anti-tyrosinase agent based on acetophenones. To increase safety and efficacy for cosmetic applications, 4-hydroxyacetophenone (**2**) was synthesized by demethylation of 4-methoxyacetophenone (**1**) using 1-dodecanethiol as an alternative reagent to minimize by-products and improve yield. The reaction conditions were optimized using BBD-RSM, with the optimum parameters being 128.8 °C, 4.00 mmol 1-dodecanethiol, and 20.75 min. Compound **2** was synthesized, purified, and spectroscopically characterized, confirming a successful demethylation reaction. Acute toxicity profiling in zebrafish showed minimal adverse effects at experimental concentrations, while depigmentation assay showed that compound **2** significantly reduced melanin levels, comparable to the positive control PTU. Tyrosinase inhibition assays showed that compound **2** had a lower IC_{50} (62.72 ± 1.39 μM) than compound **1** (IC_{50} of 143.10 ± 7.55 μM), translating compound **2** may reduce melanin via an anti-tyrosinase mechanism. Molecular docking further confirmed these findings, with compound **2** having the lowest binding affinity against both mushroom and human tyrosinase, highlighting its superior anti-tyrosinase and depigmentation potential. Overall, hydroxyl substitution at the *para*-position plays a crucial role in enhancing tyrosinase inhibition, suggesting 4-hydroxyacetophenone (**2**) as a potential lead for future anti-tyrosinase studies. Although further optimization is needed to identify candidates with the best efficacy and safety profile for cosmetic use, this study provides valuable insights and represents a significant step towards the development of effective and consumer-safe tyrosinase-targeted depigmenting agents.

Acknowledgements

This work was supported by Geran Putra Berimpak (GPB/2022/9733100). The authors would like to thank Natural Medicine and Products Research Laboratory at the Institute of Bioscience, and Department of Chemistry, Faculty of Science, Universiti Putra Malaysia, for their invaluable support and infrastructure to perform the experiments. The authors declare that they have no competing interests and confirm that no ethical approval was required for this study.

Financial disclosure

The authors have no other relevant affiliations or financial involvement with any organization or entity with a financial interest in or financial conflict with the subject matter or materials discussed in the manuscript apart from those disclosed.

Competing interest disclosure

The authors have no competing interests or relevant affiliations with any organization or entity with the subject matter or materials discussed in the manuscript. This includes employment, consultancies, honoraria, stock ownership or options, expert testimony, grants or patents received or pending, or royalties.

Writing disclosure

No writing assistance was utilized in the production of this manuscript.

References

1. França K, Keri J. Psychosocial impact of acne and postinflammatory hyperpigmentation. *An Bras Dermatol*. 92(4), 505–509 (2017).
2. Opperman L, De Kock M, Klaasen J, Rahiman F. Tyrosinase and Melanogenesis Inhibition by Indigenous African Plants: A Review. *Cosmetics*. 7(3), 60 (2020).
3. Gad SC. Hydroquinone. In: *Encyclopedia of Toxicology*, Elsevier, 425–430 (2024).
4. Nazir Y, Rafique H, Roshan S, *et al.* Molecular Docking, Synthesis, and Tyrosinase Inhibition Activity of Acetophenone Amide: Potential Inhibitor of Melanogenesis. *Biomed Res Int*. 2022(1) (2022).

5. Gheibi N, Taherkhani N, Ahmadi A, Haghbeen K, Ilghari D. Characterization of inhibitory effects of the potential therapeutic inhibitors, benzoic acid and pyridine derivatives, on the monophenolase and diphenolase activities of tyrosinase. *Iran J Basic Med Sci*. 18(2), 122–9 (2015).
6. Ait-Amir B, Pougnet P, El Hami A. Meta-Model Development. In: *Embedded Mechatronic Systems 2*, Elsevier, 151–179 (2015).
7. Chen X-K, Kwan JS-K, Chang RC-C, Ma AC-H. 1-phenyl 2-thiourea (PTU) activates autophagy in zebrafish embryos. *Autophagy*. 17(5), 1222–1231 (2021).
8. Lee J, Freeman J. Zebrafish as a Model for Developmental Neurotoxicity Assessment: The Application of the Zebrafish in Defining the Effects of Arsenic, Methylmercury, or Lead on Early Neurodevelopment. *Toxics*. 2(3), 464–495 (2014).
9. Zakaria ANN, Okello EJ, Howes M-J. Antioxidant, Anti-Collagenase, Anti-Elastase and Anti-Tyrosinase Activities of an Aqueous Cosmos caudatus Kunth (Asteraceae) Leaf Extract. *Tropical Journal of Natural Product Research*. 4(12), 1124–1130 (2021).
10. Chae J. Practical demethylation of aryl methyl ethers using an odorless thiol reagent. *Arch Pharm Res*. 31(3), 305–309 (2008).
11. Musa SH, Basri M, Masoumi HRF, *et al.* Formulation optimization of palm kernel oil esters nanoemulsion-loaded with chloramphenicol suitable for meningitis treatment. *Colloids Surf B Biointerfaces*. 112, 113–119 (2013).
12. Fard Masoumi HR, Basri M, Kassim A, *et al.* Statistical Optimization of Process Parameters for Lipase-Catalyzed Synthesis of Triethanolamine-Based Esterquats Using Response Surface Methodology in 2-Liter Bioreactor. *The Scientific World Journal*. 2013(1) (2013).
13. Song M-M, Branford-White C, Nie H-L, Zhu L-M. Optimization of adsorption conditions of BSA on thermosensitive magnetic composite particles using response surface methodology. *Colloids Surf B Biointerfaces*. 84(2), 477–483 (2011).
14. Zakaria F, Tan J-K, Mohd Faudzi SM, Abdul Rahman MB, Ashari SE. Ultrasound-assisted extraction conditions optimisation using response surface methodology from Mitragyna speciosa (Korth.) Havil leaves. *Ultrason Sonochem*. 81, 105851 (2021).
15. Zindler F, Beedgen F, Brandt D, *et al.* Analysis of tail coiling activity of zebrafish (Danio rerio) embryos allows for the differentiation of neurotoxicants with different modes of action. *Ecotoxicol Environ Saf*. 186, 109754 (2019).
16. Sampurna B, Audira G, Juniardi S, Lai Y-H, Hsiao C-D. A Simple ImageJ-Based Method to Measure Cardiac Rhythm in Zebrafish Embryos. *Inventions*. 3(2), 21 (2018).
17. Singleman C, Holtzman NG. Growth and Maturation in the Zebrafish, *Danio Rerio* : A Staging Tool for Teaching and Research. *Zebrafish*. 11(4), 396–406 (2014).
18. Russo I, Sartor E, Fagotto L, Colombo A, Tiso N, Alaibac M. The Zebrafish model in dermatology: an update for clinicians. *Discover Oncology*. 13(1), 48 (2022).
19. Qu J, Yan M, Fang Y, *et al.* Zebrafish in dermatology: a comprehensive review of their role in investigating abnormal skin pigmentation mechanisms. *Front Physiol*. 14 (2023).
20. Ryan R, Moyse BR, Richardson RJ. Zebrafish cardiac regeneration—looking beyond cardiomyocytes to a complex microenvironment. *Histochem Cell Biol*. 154(5), 533–548 (2020).

21. Lai X, Wichers HJ, Soler-López M, Dijkstra BW. Phenylthiourea Binding to Human Tyrosinase-Related Protein 1. *Int J Mol Sci*. 21(3), 915 (2020).